

1 Efficient generation of mNeonGreen *Plasmodium falciparum* reporter 2 lines enables quantitative fitness analysis

3 **Johanna Hoshizaki¹, Hannah Jagoe¹, Marcus Lee^{1*}**

4 ¹Wellcome Sanger Institute, Wellcome Genome Campus, Hinxton, Cambridge, United Kingdom

5 ***Correspondence:**

6 Marcus Lee
7 (ml31@sanger.ac.uk)

10 1 Abstract

11 CRISPR editing has enabled the rapid creation of fluorescent *Plasmodium* transgenic lines, facilitating
12 a deeper understanding of parasite biology. The impact of genetic perturbations such as gene disruption
13 or the introduction of drug resistance alleles on parasite fitness is typically quantified in competitive
14 growth assays between the query line and a wild type reference. Although fluorescent reporter lines
15 offer a facile and frequently used method to measure relative growth, this approach is limited by the
16 strain background of the existing reporter, which may not match the growth characteristics of the query
17 strains, particularly if these are slower-growing field isolates. Here, we demonstrate an efficient
18 CRISPR-based approach to generate fluorescently labelled parasite lines using mNeonGreen derived
19 from the LanYFP protein in *Branchiostoma lanceolatum*, which is one of the brightest monomeric
20 green fluorescent proteins identified. Using a positive-selection approach by insertion of an in-frame
21 blasticidin S deaminase marker, we generated a Dd2 reporter line expressing mNeonGreen under the
22 control of the *pfare* (*P. falciparum* Prodrug Activation and Resistance Esterase) locus. We selected
23 the *pfare* locus as an integration site because it is highly conserved across *P. falciparum* strains,
24 expressed throughout the intraerythrocytic cycle, not essential, and offers the potential for negative
25 selection to further enrich for integrants. The mNeonGreen@*pfare* line demonstrates strong
26 fluorescence with a negligible fitness defect. In addition, the construct developed can serve as a tool to
27 fluorescently tag other *P. falciparum* strains for *in vitro* experimentation.

28

29

30

31

32

33 **2 Introduction**

34 Transgenic parasites expressing fluorescent proteins are a powerful tool in parasitology research. The
35 ability to identify and track whole parasites or tagged parasite proteins *in vitro* has been integral for
36 gaining insights into the biology of parasites and their interactions with hosts. In the study of malaria,
37 the generation of fluorescent *Plasmodium* reporter lines has been instrumental in interrogating gene
38 function, drug activity, life cycle, and host-parasite interactions (Portugaliza et al., 2019, Thommen et
39 al., 2022, Talman et al., 2010, Frischknecht et al., 2006, Wilson et al., 2010, Voorberg-van der Wel et
40 al., 2020). Reporter lines have also been instrumental in facilitating scaled-up analyses and the
41 development of new methodologies. One important use of reporter lines is to quantify parasite fitness
42 using competitive head-to-head growth assays. A query line, typically with an engineered mutation of
43 interest such as a drug resistance allele or gene knockout, is mixed with a fluorescent isogenic wild
44 type parasite. The change in relative abundance over time provides a measure of the fitness impact of
45 the mutation of interest (Baragaña et al., 2015, Gabryszewski et al., 2016a, Ross et al., 2018, Stokes et
46 al., 2021).

47

48 The first reporter lines developed in *Plasmodium* parasites expressed the exogenous proteins, firefly
49 luciferase and chloramphenicol, using episomes (Goonewardene et al., 1993, Horrocks and Kilbey,
50 1996, Wu et al., 1995). Shortly after, green fluorescent protein (GFP) from *Aequorea victoria*, was
51 developed as a reporter and adapted into *P. falciparum* and became widely used as it provided stable
52 and strong fluorescence without requiring a cofactor (Chalfie et al., 1994, VanWye and Haldar, 1997).
53 The reporter lines enabled functional and genetic analyses, particularly the bioluminescent and
54 fluorescent reporters which supported imaging. The application of other reporters such as mCherry and
55 yellow fluorescent protein and the transition to integrated reporters were gradual and hindered by
56 challenges with homologous recombination-based integration (Engelmann et al., 2009, Armstrong and
57 Goldberg, 2007). The advent of CRISPR/Cas9 genome editing and its application in *P. falciparum*
58 made the development of reporter lines rapid and straightforward, allowing for the selective integration
59 of fluorescent markers into specific genomic sites (Mogollon et al., 2016, Kuang et al., 2017, Miyazaki
60 et al., 2020). Favourable integration sites could be selected based on the essentiality and phenotype of
61 the gene and its expression profile, allowing for the development of reporter lines with stage-specific
62 or multi-stage expression (Miyazaki et al., 2020, Marin-Mogollon et al., 2019). More recently
63 developed fluorescent proteins i.e., mNeonGreen and mGreenLantern could generate better performing
64 *Plasmodium* reporter lines as these proteins have a 3 and 6-fold increase in brightness compared to

65 mEGFP, respectively. Faster maturation, improved acid tolerance, increased photostability and
66 thermostability are also features that are often enhanced in these fluorescent proteins compared to
67 standard fluorescent proteins (Shaner et al., 2013, Campbell et al., 2020).

68

69 In this work, we developed an efficient CRISPR/Cas9 approach to generate mNeonGreen-expressing
70 *P. falciparum* lines, with the potential to use positive and negative selection to remove untagged
71 parasites and obviate the need for clonal isolation. We inserted mNeonGreen in the genome at the non-
72 essential *pfpase* (*P. falciparum* Prodrug Activation and Resistance Esterase) locus, so that its
73 integration is stable, and its expression is endogenously driven by the *pfpase* promoter. We demonstrate
74 that mNeonGreen@*pfpase* exhibits strong fluorescence throughout the intraerythrocytic cycle and has
75 robust fitness compared to existing reporter lines.

76 **3 Method**

77 **3.1 Sequence alignment**

78 DNA sequences for *pfpase* locus (PF3D7_0709700) in *P. falciparum* 3D7, HB3, 7G8, GB4, CD01,
79 GA01, IT and Dd2 strains were obtained from PlasmoDB and alignment figures were generated using
80 Clustal Omega (Amos et al., 2021, Sievers et al., 2011, Goujon et al., 2010). Transcriptomic data of
81 3D7 *pfpase* expression in the intraerythrocytic life cycle was obtained from PlasmoDB, specifically
82 RNA-sequencing data from Chappell *et al.* was used (Chappell et al., 2020).

83 **3.2 Construct design and generation**

84 The construct backbone used was pDC2-coCas9-gRNA, encoding Cas9, a gRNA expression cassette,
85 hDHFR resistance for selection for plasmid uptake in *P. falciparum* culture and ampicillin resistance
86 cassette for plasmid propagation in *E. coli* (Adjalley and Lee, 2022). Into this base vector, we inserted
87 a guide RNA targeting *pfpase* (GGACAGTCAGAAGGATGGAA), and a donor region with flanking
88 homology to 3D7 *pfpase* (255bp and 466bp homology regions; see Fig. 1B). We synthesised
89 mNeonGreen codon-optimised for *P. falciparum* and cloned this downstream of the blasticidin S
90 deaminase (BSD) selectable marker. To facilitate the expression of unfused proteins, 2A linkers were
91 included separating the upstream *pfpase* fragment, BSD, and mNeonGreen (see Fig. 1B). Cloning was
92 performed by Gibson assembly (NEBuilder DNA HiFi Assembly), and transformations were
93 performed in XL-10 Gold Ultracompetent cells (Agilent). Plasmid sequences were confirmed by

94 Sanger sequencing and plasmids were amplified and isolated using Midiprep plasmid extraction kits
95 (Macherey-Nagel).

96 **3.3 Parasite culturing and plasmid transfections**

97 Blood-stage *P. falciparum* parasites (Dd2, Dd2-EGFP and NF54-EGFP) were grown in RPMI media
98 with AlbuMAX® (Gibco) and supplemented with GlutaMax® (Gibco), Gentamicin (Gibco) and
99 HEPES (pH 7.0) with O+ human erythrocytes at 3% haematocrit. RBCs were obtained by anonymous
100 donors from the National Health Services Blood and Transplant (NHSBT). Their use was in accordance
101 with relevant guidelines and regulations, with approval from the NHS Cambridgeshire Research Ethics
102 Committee and the Wellcome Sanger Institute Human Materials and Data Management Committee.
103 Cultures were maintained in a gaseous environment of 3% CO₂, 1% O₂ and 96% N₂ at 37°C.
104 Parasitemia and stages were monitored using Giemsa staining and microscopy. Synchronisation was
105 completed using sorbitol ring enrichment (Radfar et al., 2009). Transfections were completed by
106 electroporation of parasitised red blood cells (Bio-Rad Gene Pulser Xcell) as previously described
107 (Fidock and Wellem, 1997). Cultures containing 5% ring-stage parasites were transfected with 50µg
108 of the plasmid. Blasticidin S drug selection (2µg/ml) was applied one-day post-electroporation and
109 maintained continuously. Correct editing of recrudesced parasites (mNeonGreen@*pare.1* and
110 mNeonGreen@*pare.2*) was confirmed using primers (p2174 and p2175), which flank the 5' and 3'
111 UTRs of *pfpf* (TGCACTTGTTCACATTTTATATT and
112 TGTAACATCACTAATTAAATTATTAA). PCR amplification and gel electrophoresis were used to
113 check insert size and Sanger sequencing to confirm the correct sequence. The Dd2-EGFP and NF54-
114 EGFP fluorescent lines were previously published (Baragaña et al., 2015, Gabryszewski et al., 2016b).
115 Both lines were generated using attB x attP recombination to insert the reporter genes, however, they
116 are driven by different constitutive promoters: Dd2-EGFP is driven by the ER hsp70
117 (PF3D7_0917900) promoter and the NF54-EGFP by the calmodulin (PF3D7_1434200) promoter.

118 **3.4 Fluorescence microscopy**

119 200µL of parasite culture was harvested at 5% parasitemia, spun at 3000rpm for 30 seconds in an
120 Eppendorf tube and washed with 0.5mL of PBS. Parasites were fixed by resuspending in 4% (v/v)
121 paraformaldehyde + 0.0075% glutaraldehyde, incubating for 30 minutes, and washed twice with 1mL
122 of PBS. Parasite DNA was stained with 1mL of Hoechst stain (10µg/mL) for 5 minutes and
123 resuspended in 1mL of PBS. The stained parasites were transferred to an 8-well chambered coverglass

124 (Lab-Tek) pre-treated with 0.25mL of poly L-lysine (0.2mg/ml) for 10mins. The coverglass was
125 transferred to an inverted fluorescence microscope (Leica DMi8). Bright-field microscopy and blue
126 and green-filtered fluorescence microscopy were used with the 100x objective (total 1000x
127 magnification) to image infected erythrocytes and fluorescent parasites. Image processing and analysis
128 were completed with Leica Application Suite (LAS X).

129 **3.5 Flow cytometric analysis of fluorescence**

130 Parasites were transferred to a round-bottom 96-well plate, spun (3min s, 2000rpm) and the supernatant
131 was removed. To check viability, infected erythrocytes were stained with 100nM MitoTracker Deep
132 Red (MitoDR) solution (Thermofisher) in NaCl 0.9%/Dextrose 0.2% and incubated for 30mins in the
133 dark at 37°C. After a 1/40 dilution in PBS, parasites were analysed on a flow cytometer (Beckman
134 Coulter CytoFLEX S) and at least 20 000 events were recorded for each experiment. The blue 488nm
135 laser was used to detect green fluorescence and the red 638nm laser was used to detect MitoDR.
136 Quantification of green fluorescent (GFP and mNeonGreen) and MitoDR positive cells in the culture
137 population was performed using FlowJo (v10).

138 **3.6 Competition assay**

139 Pre-assay parasitemia was measured using flow cytometry and stages were observed with microscopy.
140 Mixed-stage lines of mNeonGreen@*pare*.1, mNeonGreen@*pare*.2 and Dd2-EGFP were competed
141 against Dd2 or 3D7 in triplicate at 50:50 starting ratio with a total of 1% parasitemia. The parasitemia
142 and fluorescence were measured using flow cytometry every 2nd or 3rd day from day 0 to day 21.
143 Parasitemia was maintained between 0.5%-6%. The percentage of parasites expressing green
144 fluorescence over total parasites was averaged between the triplicates and graphed over time for each
145 line.

146 **4 Results**

147 **4.1 Selection of the *pfp* locus for fluorescent markers integration in *P. falciparum***

148 The *pfp* locus was identified as an optimal safe-harbour site for the integration of the mNeonGreen
149 fluorescent marker. *pfp* (PF3D7_0709700) encodes a prodrug activation and resistance esterase that
150 is not essential (Istvan et al., 2017). In addition to the dispensable nature of *pfp*, loss-of-function
151 mutations in *pfp* confer resistance to the antimalarial compound MMV011438, which requires
152 *pfp* for its activation. *pfp* is expressed during blood stages, therefore its promoter would facilitate

153 the expression of a fluorescent marker throughout the intraerythrocytic life cycle. In addition, we
154 included in the inserted sequence the blasticidin S deaminase (BSD) marker, which would only be
155 expressed from the *pfp*are promoter once integrated. Thus our strategy would permit both positive and
156 negative selection options if required for efficient isolation of a homogenous culture of mNeonGreen
157 tagged parasites without cloning.

158

159 To identify if *pfp*are is suitable as an integration site across multiple *P. falciparum* strains, a multiple
160 sequence alignment of the *pfp*are locus for eight geographically diverse strains (3D7, HB3, 7G8, GB4,
161 CD01, GA01, IT and Dd2) was completed. We first identified a gRNA target site that was highly
162 conserved, with no mutations in the guide RNA or PAM sequences (Fig. 1A). Examination of the
163 flanking upstream and downstream sequences that would constitute the donor homology regions
164 revealed no mutations in the 5' homology region and 2 – 3 single nucleotide polymorphisms in the 3'
165 homology region of the donor sequence of the plasmid (Supplemental Fig. 1). This level of sequence
166 diversity would not be expected to strongly impact editing. We validated this prediction below using a
167 3D7-based donor sequence to edit Dd2, which has three polymorphisms relative to 3D7.

168 4.2 Generation of an endogenous mNeonGreen-expressing *P. falciparum* reporter line

169 To design a construct to integrate mNeonGreen into *pfp*are, we first subcloned a codon-optimised
170 mNeonGreen downstream of BSD, with flanking 5' and 3' *pfp*are (3D7) homology regions of 255 bp
171 and 466 bp respectively. The resulting plasmid (pDC-coCas9-*pfp*are-BSD-mNeonGreen; Fig. 1B)
172 expresses Cas9 driven by the calmodulin promoter and transcribes a *pfp*are-targeting guide RNA.
173 Plasmids were transfected into *P. falciparum* Dd2 parasites and continuous selection with blasticidin
174 S was used to select for plasmid uptake and the insertion of the donor into *pfp*are by homology-directed
175 repair (Fig. 1C). Edited parasites were obtained from two different transfections, referred to as
176 mNeonGreen@*pfp*are.1 and mNeonGreen@*pfp*are.2. PCR-amplification of the *pfp*are locus demonstrated
177 successful integration of the donor with no wild type locus detectable, indicating positive selection was
178 sufficient to deplete any unedited parasites (Fig. 1D, primers shown in Fig. 1C).

179 4.3 Endogenous mNeonGreen expression generates fluorescence comparable to GFP

180 To determine if the integrated mNeonGreen yields fluorescent parasites, we first examined the
181 transgenic lines by fluorescence microscopy. Infected erythrocytes were detected using Hoechst DNA
182 stain, which does not stain uninfected erythrocytes because they are anucleate, unlike *Plasmodium*

183 parasites. Erythrocytes infected with either of the mNeonGreen@*pare* lines showed strong green
184 fluorescence unlike the parental Dd2 line (Fig. 2A). Flow cytometry was used to quantify the level of
185 fluorescence and distribution within the population of a mixed-stage culture. The fluorescence profiles
186 of mNeonGreen@*pare*.1 and mNeonGreen@*pare*.2 were highly similar and are comparable to the
187 profiles of other green-fluorescing lines used for competition assays, including Dd2-EGFP and NF54-
188 EGFP, which express GFP from the strong constitutive promoters of ER-Hsp70 and calmodulin
189 respectively (Adjalley et al., 2010, Baragaña et al., 2015). The peaks of the mNeonGreen@*pare* lines
190 were modestly shifted left in comparison to the GFP lines, which means that the bulk of
191 mNeonGreen@*pare* parasites in mixed culture are less fluorescent than the bulk of GFP-expressing
192 parasites but still readily distinguishable from non-fluorescent parasites (Fig. 2B). The bimodal peaks
193 suggested that subpopulations expressed different levels of fluorescence.

194 **4.4 mNeonGreen fluorescence varies between different asexual *P. falciparum* blood stages**

195 In a healthy asexual intraerythrocytic *P. falciparum* culture, the subpopulations include briefly free-
196 roaming merozoites and intraerythrocytic ring, trophozoite and schizont stages. To assess the level of
197 fluorescence in specific stages, we enriched mNeonGreen@*pare* cultures for different stages using
198 synchronisation. Stage-specific levels of fluorescence were observed with schizonts producing the
199 highest fluorescence, followed by trophozoites and lastly, ring stages (Fig. 3A). This pattern was
200 consistent with transcriptomic studies that demonstrate that the expression of *pfpf* peaks at 32-40
201 hours post-erythrocyte-invasion, which would suggest that the expression of mNeonGreen from the
202 *pfpf* locus would also peak during late trophozoite and schizont stages (Fig 3B) (Chappell et al.,
203 2020, Amos et al., 2021).

204 **4.5 mNeonGreen@*pare* lines demonstrate robust fitness**

205 To assess the fitness of the mNeonGreen@*pare* lines, competition assays were performed against Dd2
206 and 3D7. The two populations were seeded at a 1:1 ratio of fluorescent to test line and maintained for
207 3 weeks. The ratio of fluorescent (mNeonGreen@*pare*) to non-fluorescent (Dd2 or 3D7) populations
208 was measured every 2 - 3 days using flow cytometry to quantify the competition between the two
209 populations. Dd2-EGFP was also included as a control, which has been shown previously to have a
210 slight fitness defect due to the integration of GFP (Baragaña et al., 2015). The mNeonGreen@*pare*
211 lines showed nearly comparable fitness to their parent line, Dd2, over a three-week period (Fig. 4A).

212 Contrastingly when competed against 3D7, a slower-growing lab line, the mNeonGreen@*pare* lines
213 outcompeted 3D7, which demonstrates the value of strain-matched competitor lines (Fig. 4B).

214 **5 Discussion**

215 Genetic engineering of fluorescent proteins has greatly improved their functionality as tools in
216 molecular biology. As such the integration of these enhanced proteins into existing applications in
217 malaria research should be explored. In this work, we have developed an efficient and facile approach
218 for generating new fluorescent reporter lines in *P. falciparum* using CRISPR-based integration of
219 mNeonGreen. mNeonGreen was first applied to *P. falciparum* to generate a tagged Exp2 protein
220 however, here we aimed to assess its broader applicability in generating reporter lines for competitive
221 fitness assays (Glushakova et al., 2018). Therefore, we designed a CRISPR/Cas9 construct to integrate
222 mNeonGreen into *pfare*, a highly conserved, nonessential gene that would endogenously drive
223 expression throughout the intraerythrocytic cycle.

224

225 We used the construct to tag the Dd2 strain and then assessed mNeonGreen@*pare* for features suitable
226 in a reporter line i.e., the strength of fluorescence, localisation, stage-specificity, and impact on parasite
227 fitness. mNeonGreen@*pare* demonstrated strong fluorescence that was diffused throughout the
228 parasite. The fluorescence was expressed in all asexual blood stages but was most concentrated in
229 schizonts. The ability to efficiently tag Dd2 indicates that minor differences in the homology regions
230 between the donor, based on the 3D7 sequence, and the target region are tolerated. The absence of wild
231 type locus in bulk transfections reflects the effect of positive selection resulting from *bsd* expression
232 from the endogenous *pfare* promoter. Although disruption of *pfare* also affords the possibility of
233 negative selection using the commercially available compound MMV011438, this was not required in
234 practice due to the stringency of the blasticidin S positive selection. The integration of mNeonGreen
235 into *pfare* caused a minor fitness defect leading to slightly slower growth compared to Dd2, similar
236 to other GFP-based reporters (Baragaña et al., 2015). However, this defect was relatively minimal, as
237 the resulting line outcompeted 3D7 in a competition assay. These findings support that the
238 mNeonGreen@*pare* is a suitable reporter line and is comparable with the standard *P. falciparum* GFP
239 lines that are currently used.

240

241 Both tools generated in this work, the Dd2 mNeonGreen reporter line and the construct that generates
242 new reporter lines, will support malaria research. mNeonGreen@*pare* is a valuable addition to the

243 repertoire of reporter lines in *P. falciparum* that facilitate experiments involving visualising, tracking
244 and counting parasites. The pDC-coCas9-*pare*-BSD-mNeonGreen construct will enable the rapid
245 generation of other fluorescently tagged *P. falciparum* parasites from different strains, such as field
246 isolates, which can facilitate their study *in vitro*.

247 **6 Conflict of Interest**

248 The authors declare that the research was conducted in the absence of any commercial or financial
249 relationships that could be construed as a potential conflict of interest.

250 **7 Author Contributions**

251 JH and ML conceived and designed the experiments. HJ generated the pDC2-coCas9-*pare*-2A-BSD
252 construct. JH generated the pDC-coCas9-*pare*-BSD-mNeonGreen plasmid and performed the
253 experiments and analysis. ML supervised the work. JH and ML wrote the manuscript. All authors read
254 and approved the manuscript.

255 **8 Funding**

256 This research was funded by the Wellcome Trust [grant 206194].

257 **9 References**

258 Adjalley, S. H. & Lee, M. C. 2022. CRISPR/Cas9 editing of the *Plasmodium falciparum* genome.
259 *Methods in Molecular Biology*.

260 Adjalley, S. H., Lee, M. C. & Fidock, D. A. 2010. A method for rapid genetic integration into
261 *Plasmodium falciparum* utilizing mycobacteriophage Bxb1 integrase. *Methods Mol Biol*, 634,
262 87-100.

263 Amos, B., Aurrecoechea, C., Barba, M., Barreto, A., Basenko, Evelina y., Bažant, W., Belnap, R.,
264 Blevins, A. S., Böhme, U., Brestelli, J., Brunk, B. P., Caddick, M., Callan, D., Campbell, L.,
265 Christensen, Mikkel b., Christophides, George k., Crouch, K., Davis, K., Debarry, J.,
266 Doherty, R., Duan, Y., Dunn, M., Falke, D., Fisher, S., Flicek, P., Fox, B., Gajria, B.,
267 Giraldo-Calderón, G. I., Harb, O. S., Harper, E., Hertz-Fowler, C., Hickman, Mark j.,
268 Howington, C., Hu, S., Humphrey, J., Iodice, J., Jones, A., Judkins, J., Kelly, S. A., Kissinger,
269 J. C., Kwon, D. K., Lamoureux, K., Lawson, D., Li, W., Lies, K., Lodha, D., Long, J.,
270 Maccallum, R. M., Maslen, G., McDowell, M. A., Nabrzyski, J., Roos, D. S., Rund, S. S. C.,
271 Schulman, Stephanie w., Shanmugasundram, A., Sitnik, V., Spruill, D., Starns, D., Stoeckert,
272 Christian j., Jr, Tomko, S. S., Wang, H., Warrenfeltz, S., Wieck, R., Wilkinson, P. A., Xu, L.
273 & Zheng, J. 2021. VEuPathDB: the eukaryotic pathogen, vector and host bioinformatics
274 resource center. *Nucleic Acids Research*, 50, D898-D911.

275 Armstrong, C. M. & Goldberg, D. E. 2007. An FKBP destabilization domain modulates protein
276 levels in *Plasmodium falciparum*. *Nat Methods*, 4, 1007-9.

277 Baragaña, B., Hallyburton, I., Lee, M. C., Norcross, N. R., Grimaldi, R., Otto, T. D., Proto, W. R.,
278 Blagborough, A. M., Meister, S., Wirjanata, G., Ruecker, A., Upton, L. M., Abraham, T. S.,
279 Almeida, M. J., Pradhan, A., Porzelle, A., Luksch, T., Martínez, M. S., Luksch, T., Bolscher,
280 J. M., Woodland, A., Norval, S., Zuccotto, F., Thomas, J., Simeons, F., Stojanovski, L.,
281 Osuna-Cabello, M., Brock, P. M., Churcher, T. S., Sala, K. A., Zakutansky, S. E., Jiménez-
282 Díaz, M. B., Sanz, L. M., Riley, J., Basak, R., Campbell, M., Avery, V. M., Sauerwein, R.
283 W., Dechering, K. J., Noviyanti, R., Campo, B., Frearson, J. A., Angulo-Barturen, I., Ferrer-
284 Bazaga, S., Gamo, F. J., Wyatt, P. G., Leroy, D., Siegl, P., Delves, M. J., Kyle, D. E., Wittlin,
285 S., Marfurt, J., Price, R. N., Sinden, R. E., Winzeler, E. A., Charman, S. A., Bebrevska, L.,
286 Gray, D. W., Campbell, S., Fairlamb, A. H., Willis, P. A., Rayner, J. C., Fidock, D. A., Read,
287 K. D. & Gilbert, I. H. 2015. A novel multiple-stage antimalarial agent that inhibits protein
288 synthesis. *Nature*, 522, 315-20.

289 Campbell, B. C., Nabel, E. M., Murdock, M. H., Lao-Peregrin, C., Tsoulfas, P., Blackmore, M. G.,
290 Lee, F. S., Liston, C., Morishita, H. & Petsko, G. A. 2020. mGreenLantern: a bright
291 monomeric fluorescent protein with rapid expression and cell filling properties for neuronal
292 imaging. *Proc Natl Acad Sci U S A*, 117, 30710-30721.

293 Chalfie, M., Tu, Y., Euskirchen, G., Ward, W. W. & Prasher, D. C. 1994. Green Fluorescent Protein
294 as a Marker for Gene Expression. *Science*, 263, 802-805.

295 Chappell, L., Ross, P., Orchard, L., Russell, T. J., Otto, T. D., Berriman, M., Rayner, J. C. & Llinás,
296 M. 2020. Refining the transcriptome of the human malaria parasite *Plasmodium falciparum*
297 using amplification-free RNA-seq. *BMC Genomics*, 21, 395.

298 Engelmann, S., Silvie, O. & Matuschewski, K. 2009. Disruption of *Plasmodium* sporozoite
299 transmission by depletion of sporozoite invasion-associated protein 1. *Eukaryot Cell*, 8, 640-
300 8.

301 Fidock, D. A. & Wellem, T. E. 1997. Transformation with human dihydrofolate reductase renders
302 malaria parasites insensitive to WR99210 but does not affect the intrinsic activity of
303 proguanil. *Proc Natl Acad Sci U S A*, 94, 10931-6.

304 Frischknecht, F., Martin, B., Thiery, I., Bourgouin, C. & Menard, R. 2006. Using green fluorescent
305 malaria parasites to screen for permissive vector mosquitoes. *Malaria Journal*, 5, 23.

306 Gabryszewski, S. J., Dhingra, S. K., Combrinck, J. M., Lewis, I. A., Callaghan, P. S., Hassett, M. R.,
307 Siriwardana, A., Henrich, P. P., Lee, A. H., Gnädig, N. F., Musset, L., Llinás, M., Egan, T. J.,
308 Roepe, P. D. & Fidock, D. A. 2016a. Evolution of Fitness Cost-Neutral Mutant PfCRT
309 Conferring *P. falciparum* 4-Aminoquinoline Drug Resistance Is Accompanied by Altered
310 Parasite Metabolism and Digestive Vacuole Physiology. *PLoS Pathog*, 12, e1005976.

311 Gabryszewski, S. J., Modchang, C., Musset, L., Chookajorn, T. & Fidock, D. A. 2016b.
312 Combinatorial Genetic Modeling of pf crt-Mediated Drug Resistance Evolution in
313 *Plasmodium falciparum*. *Molecular Biology and Evolution*, 33, 1554-1570.

314 Glushakova, S., Beck, J. R., Garten, M., Busse, B. L., Nasamu, A. S., Tenkova-Heuser, T., Heuser,
315 J., Goldberg, D. E. & Zimmerberg, J. 2018. Rounding precedes rupture and breakdown of
316 vacuolar membranes minutes before malaria parasite egress from erythrocytes. *Cell
317 Microbiol*, 20, e12868.

318 Goonewardene, R., Daily, J., Kaslow, D., Sullivan, T. J., Duffy, P., Carter, R., Mendis, K. & Wirth,
319 D. 1993. Transfection of the malaria parasite and expression of firefly luciferase. *Proc Natl
320 Acad Sci U S A*, 90, 5234-6.

321 Goujon, M., Mcwilliam, H., Li, W., Valentin, F., Squizzato, S., Paern, J. & Lopez, R. 2010. A new
322 bioinformatics analysis tools framework at EMBL-EBI. *Nucleic Acids Research*, 38, W695-
323 W699.

324 Horrocks, P. & Kilbey, B. J. 1996. Physical and functional mapping of the transcriptional start sites
325 of *Plasmodium falciparum* proliferating cell nuclear antigen. *Mol Biochem Parasitol*, 82, 207-
326 15.

327 Istvan, E. S., Mallari, J. P., Corey, V. C., Dharia, N. V., Marshall, G. R., Winzeler, E. A. &
328 Goldberg, D. E. 2017. Esterase mutation is a mechanism of resistance to antimalarial
329 compounds. *Nature Communications*, 8, 14240.

330 Kuang, D., Qiao, J., Li, Z., Wang, W., Xia, H., Jiang, L., Dai, J., Fang, Q. & Dai, X. 2017. Tagging
331 to endogenous genes of *Plasmodium falciparum* using CRISPR/Cas9. *Parasit Vectors*, 10,
332 595.

333 Marin-Mogollon, C., Salman, A. M., Koolen, K. M. J., Bolscher, J. M., Van Pul, F. J. A., Miyazaki,
334 S., Imai, T., Othman, A. S., Ramesar, J., Van Gemert, G. J., Kroeze, H., Chevalley-Maurel,
335 S., Franke-Fayard, B., Sauerwein, R. W., Hill, A. V. S., Dechering, K. J., Janse, C. J. & Khan,
336 S. M. 2019. A *P. falciparum* NF54 Reporter Line Expressing mCherry-Luciferase in
337 Gametocytes, Sporozoites, and Liver-Stages. *Front Cell Infect Microbiol*, 9, 96.

338 Miyazaki, S., Yang, A. S. P., Geurten, F. J. A., Marin-Mogollon, C., Miyazaki, Y., Imai, T., Kolli, S.
339 K., Ramesar, J., Chevalley-Maurel, S., Salman, A. M., Van Gemert, G. A., Van
340 Waardenburg, Y. M., Franke-Fayard, B., Hill, A. V. S., Sauerwein, R. W., Janse, C. J. &
341 Khan, S. M. 2020. Generation of Novel *Plasmodium falciparum* NF135 and NF54 Lines
342 Expressing Fluorescent Reporter Proteins Under the Control of Strong and Constitutive
343 Promoters. *Front Cell Infect Microbiol*, 10, 270.

344 Mogollon, C. M., Van Pul, F. J., Imai, T., Ramesar, J., Chevalley-Maurel, S., De Roo, G. M., Veld,
345 S. A., Kroeze, H., Franke-Fayard, B. M., Janse, C. J. & Khan, S. M. 2016. Rapid Generation
346 of Marker-Free *P. falciparum* Fluorescent Reporter Lines Using Modified CRISPR/Cas9
347 Constructs and Selection Protocol. *PLoS One*, 11, e0168362.

348 Portugaliza, H. P., Llorà-Batlle, O., Rosanas-Urgell, A. & Cortés, A. 2019. Reporter lines based on
349 the gexp02 promoter enable early quantification of sexual conversion rates in the malaria
350 parasite *Plasmodium falciparum*. *Scientific Reports*, 9, 14595.

351 Radfar, A., Méndez, D., Moneriz, C., Linares, M., Marín-García, P., Puyet, A., Diez, A. & Bautista,
352 J. M. 2009. Synchronous culture of *Plasmodium falciparum* at high parasitemia levels. *Nature
353 Protocols*, 4, 1899-1915.

354 Ross, L. S., Dhingra, S. K., Mok, S., Yeo, T., Wicht, K. J., Kumpornsin, K., Takala-Harrison, S.,
355 Witkowski, B., Fairhurst, R. M., Ariey, F., Menard, D. & Fidock, D. A. 2018. Emerging
356 Southeast Asian PfCRT mutations confer *Plasmodium falciparum* resistance to the first-line
357 antimalarial piperaquine. *Nat Commun*, 9, 3314.

358 Shaner, N. C., Lambert, G. G., Chammas, A., Ni, Y., Cranfill, P. J., Baird, M. A., Sell, B. R., Allen,
359 J. R., Day, R. N., Israelsson, M., Davidson, M. W. & Wang, J. 2013. A bright monomeric
360 green fluorescent protein derived from *Branchiostoma lanceolatum*. *Nat Methods*, 10, 407-9.

361 Sievers, F., Wilm, A., Dineen, D., Gibson, T. J., Karplus, K., Li, W., Lopez, R., Mcwilliam, H.,
362 Remmert, M., Söding, J., Thompson, J. D. & Higgins, D. G. 2011. Fast, scalable generation
363 of high-quality protein multiple sequence alignments using Clustal Omega. *Molecular
364 Systems Biology*, 7, 539.

365 Stokes, B. H., Dhingra, S. K., Rubiano, K., Mok, S., Straimer, J., Gnädig, N. F., Deni, I., Schindler,
366 K. A., Bath, J. R., Ward, K. E., Striepen, J., Yeo, T., Ross, L. S., Legrand, E., Ariey, F.,
367 Cunningham, C. H., Souleymane, I. M., Gansané, A., Nzoumbou-Boko, R., Ndayikunda, C.,
368 Kabanywanyi, A. M., Uwimana, A., Smith, S. J., Kolley, O., Ndounga, M., Warsame, M.,
369 Leang, R., Nosten, F., Anderson, T. J., Rosenthal, P. J., Ménard, D. & Fidock, D. A. 2021.
370 *Plasmodium falciparum* K13 mutations in Africa and Asia impact artemisinin resistance and
371 parasite fitness. *Elife*, 10.

372 Talman, A. M., Blagborough, A. M. & Sinden, R. E. 2010. A *Plasmodium falciparum* strain
373 expressing GFP throughout the parasite's life-cycle. *PLoS One*, 5, e9156.
374 Thommen, B. T., Passeecker, A., Buser, T., Hitz, E., Voss, T. S. & Brancucci, N. M. B. 2022.
375 Revisiting the Effect of Pharmaceuticals on Transmission Stage Formation in the Malaria
376 Parasite *Plasmodium falciparum*. *Frontiers in Cellular and Infection Microbiology*, 12.
377 Vanwye, J. D. & Haldar, K. 1997. Expression of green fluorescent protein in *Plasmodium*
378 *falciparum*. *Mol Biochem Parasitol*, 87, 225-9.
379 Voorberg-Van Der Wel, A. M., Zeeman, A.-M., Nieuwenhuis, I. G., Van Der Werff, N. M., Klooster,
380 E. J., Klop, O., Vermaat, L. C., Kumar Gupta, D., Dembele, L., Diagana, T. T. & Kocken, C.
381 H. M. 2020. A dual fluorescent *Plasmodium cynomolgi* reporter line reveals in vitro malaria
382 hypnozoite reactivation. *Communications Biology*, 3, 7.
383 Wilson, D. W., Crabb, B. S. & Beeson, J. G. 2010. Development of fluorescent *Plasmodium*
384 *falciparum* for in vitro growth inhibition assays. *Malaria Journal*, 9, 152.
385 Wu, Y., Sifri, C. D., Lei, H. H., Su, X. Z. & Wellem, T. E. 1995. Transfection of *Plasmodium*
386 *falciparum* within human red blood cells. *Proc Natl Acad Sci U S A*, 92, 973-7.

387 **10 Figure Legends**

388 **Figure 1. Generation of a *P. falciparum* Dd2 reporter line expressing mNeonGreen under the**
389 **control of the highly conserved *pfpf* locus (mNeonGreen@pare).** (A) DNA sequences for *pfpf*
390 (PF3D7_0709700) in *P. falciparum* 3D7, HB3, 7G8, GB4, CD01, GA01, IT and Dd2 strains were
391 obtained from PlasmoDB and Clustal Omega was used to create a multiple sequence alignment (Amos
392 et al., 2021, Sievers et al., 2011, Goujon et al., 2010). (B) Schematic of the pDC2-coCas9-*pfpf*-BSD-
393 mNeonGreen plasmid. The plasmid encodes a codon optimised Cas9 enzyme, guide RNA cassette
394 containing a guide targeting *pfpf*, an ampicillin resistance cassette for plasmid propagation in *E. coli*
395 and the hDHFR marker for selection for plasmid uptake in *P. falciparum*. The donor region contains a
396 blasticidin S deaminase (BSD) selectable marker flanked by 2A linkers with mNeonGreen
397 downstream. The payload is flanked by two homology regions for the *pfpf* locus. (C) Upon
398 transfection of the pDC2-coCas9-*pfpf*-BSD-mNeonGreen plasmid into *P. falciparum* Dd2, the *pfpf*-
399 targeting gRNA directs Cas9 to make a site-directed cut of *pfpf*. The donor region facilitates
400 homology-directed repair and the insertion of BSD and mNeonGreen. (D) The *pfpf* locus of
401 blasticidin-resistant recrudescing parasites (mNeonGreen@pare.1 and mNeonGreen@pare.2) was
402 PCR-amplified using 5' and 3' UTR primers (p2174 and p2175) to check for correct insertion of
403 mNeonGreen. Lengths of PCR products were quantified using gel electrophoresis. No detectable wild
404 type product was observed in the transfected bulk culture.

405 **Figure 2. mNeonGreen fluorescence in *P. falciparum* is comparable to GFP fluorescent lines.** (A)
406 Mixed-staged parasites (mNeonGreen@pare.1, mNeonGreen@pare.2, Dd2, NF54-EGFP, Dd2-
407 EGFP) were fixed using 4% (v/v) paraformaldehyde + 0.0075% glutaraldehyde, stained with Hoechst
408 stain, and placed on a poly L-lysine coated coverglass for inverted fluorescence microscopy. Bright-
409 field microscopy and fluorescence microscopy were used with a 100x objective (total 1000x
410 magnification) and with green and blue fluorescence was captured to image infected RBCs and
411 fluorescent parasites. (B) Mixed-stage parasites (mNeonGreen@pare.1, mNeonGreen@pare.2, Dd2,
412 NF54-EGFP, Dd2-EGFP) were stained with MitoTracker DeepRed and analysed on a flow cytometer.
413 Quantification of green fluorescent (GFP and mNeonGreen) and MitoTracker⁺ cells was performed
414 using FlowJo. All single-cell, parasitised RBCs (MitoTracker⁺) were gated, and histograms of green
415 fluorescence were generated (GFP⁺ or mNeonGreen⁺).
416

417

418 **Figure 3. mNeonGreen@*pare* fluorescence varies between different asexual blood stages.** (A)
419 mNeonGreen@*pare*.2 parasites were synchronised using sorbitol ring-stage enrichment and
420 microscopy was used to confirm stages. Flow cytometry with MitoTracker DeepRed was used to
421 enumerate parasites expressing green fluorescence in ring, trophozoite and schizont-staged cultures.
422 FlowJo was used to gate single-cell, parasitised RBCs, quantify green fluorescence, and generate
423 histograms. mNeonGreen@*pare* schizonts demonstrated the greatest fluorescence followed by
424 trophozoites and then rings. (B) Stage-specific RNA-sequencing obtained from PlasmoDB shows that
425 *pfpf* is expressed throughout the entire 48hr intraerythrocytic life cycle and expression peaks at late
426 trophozoite and schizont stages (Amos et al., 2021, Chappell et al., 2020).

427

428 **Figure 4. mNeonGreen@*pare* lines demonstrate comparable fitness to Dd2-EGFP when**
429 **competed against Dd2 or 3D7.** Fluorescent lines (mNeonGreen@*pare*.1, mNeonGreen@*pare*.2 and
430 Dd2-EGFP) were competed against (A) Dd2 or (B) 3D7 in triplicate. The two populations were seeded
431 at a 1:1 ratio at 1% parasitemia and maintained for 3 weeks. The parasitemia and fluorescence were
432 measured using flow cytometry every 2nd or 3rd day from day 0 to day 21. The percentage of green
433 fluorescent parasites over total parasites was averaged between the triplicates and graphed over time
434 for each line. In the competition assay vs. Dd2, the three fluorescent lines did not outcompete Dd2 and
435 remained close to the seeded percentages over three weeks. However, in the competition assay vs. 3D7,
436 the three fluorescent lines quickly outcompeted 3D7.

437

438 **Supplemental Figure 1. Alignment of 5' and 3' homologous regions of the *pfpf* locus in *P.***
439 ***falciparum* sequences.** The DNA sequences of the 5' (A) and 3' (B) *pfpf* homologous regions used
440 in pDC2-coCas9-*pare*-BSD-mNeonGreen were obtained for *P. falciparum* 3D7, HB3, 7G8, GB4,
441 CD01, GA01, IT and Dd2 strains from PlasmoDB (Amos et al., 2021). Clustal Omega was used to
442 create a multiple sequence alignment (Sievers et al., 2011, Goujon et al., 2010). Single nucleotide
443 polymorphisms are highlighted with yellow boxes.

444

Figure 1

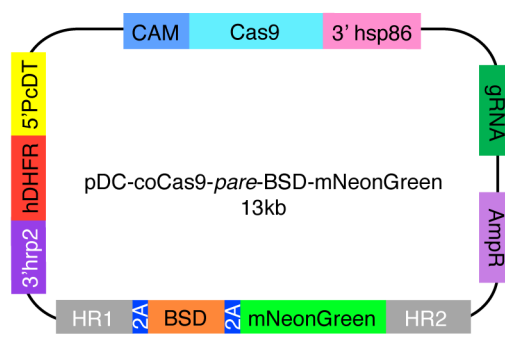
A

gRNA PAM

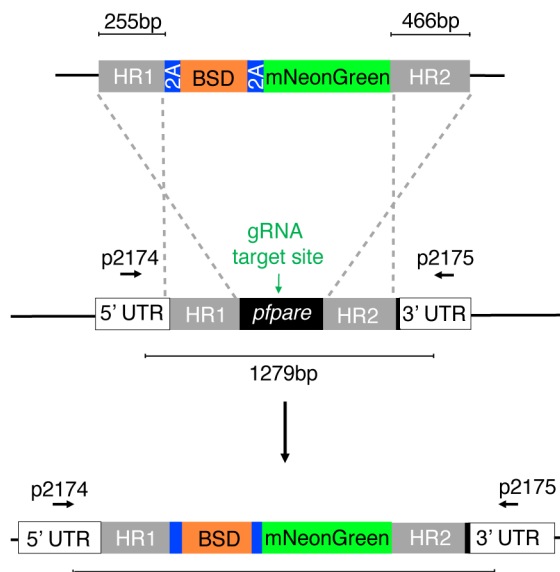
```

3D7 321 TGGAATAGATTACAAAGTCATGGACAGTCAGAAGGATGGAAAGGTTAAGAACCCATATAAGACAATTGATGATATAG 400
CD01 321 TGGAATAGATTACAAAGTCATGGACAGTCAGAAGGATGGAAAGGTTAAGAACCCATATAAGACAATTGATGATATAG 400
7G8 321 TGGAATAGATTACAAAGTCATGGACAGTCAGAAGGATGGAAAGGTTAAGAACCCATATAAGACAATTGATGATATAG 400
HB3 321 TGGAATAGATTACAAAGTCATGGACAGTCAGAAGGATGGAAAGGTTAAGAACCCATATAAGACAATTGATGATATAG 400
GA01 321 TGGAATAGATTACAAAGTCATGGACAGTCAGAAGGATGGAAAGGTTAAGAACCCATATAAGACAATTGATGATATAG 400
GB4 321 TGGAATAGATTACAAAGTCATGGACAGTCAGAAGGATGGAAAGGTTAAGAACCCATATAAGACAATTGATGATATAG 400
IT 321 TGGAATAGATTACAAAGTCATGGACAGTCAGAAGGATGGAAAGGTTAAGAACCCATATAAGACAATTGATGATATAG 400
Dd2 321 TGGAATAGATTACAAAGTCATGGACAGTCAGAAGGATGGAAAGGTTAAGAACCCATATAAGACAATTGATGATATAG 400
*****
```

B



C



D

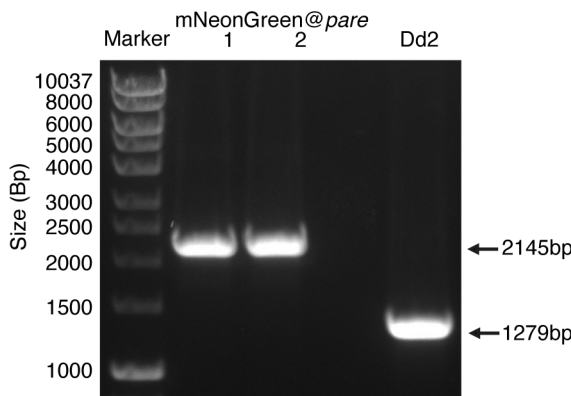


Figure 2

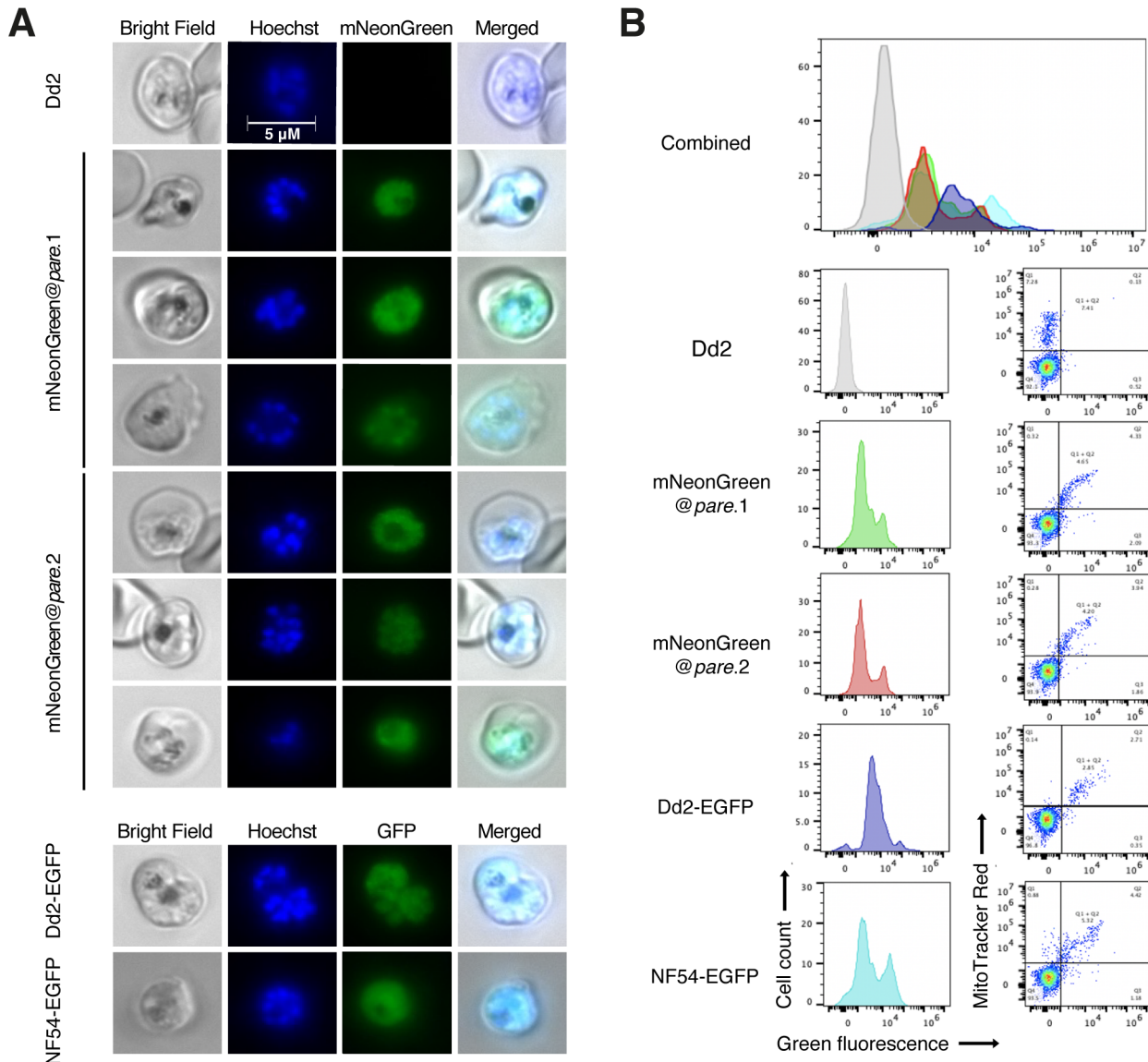


Figure 3

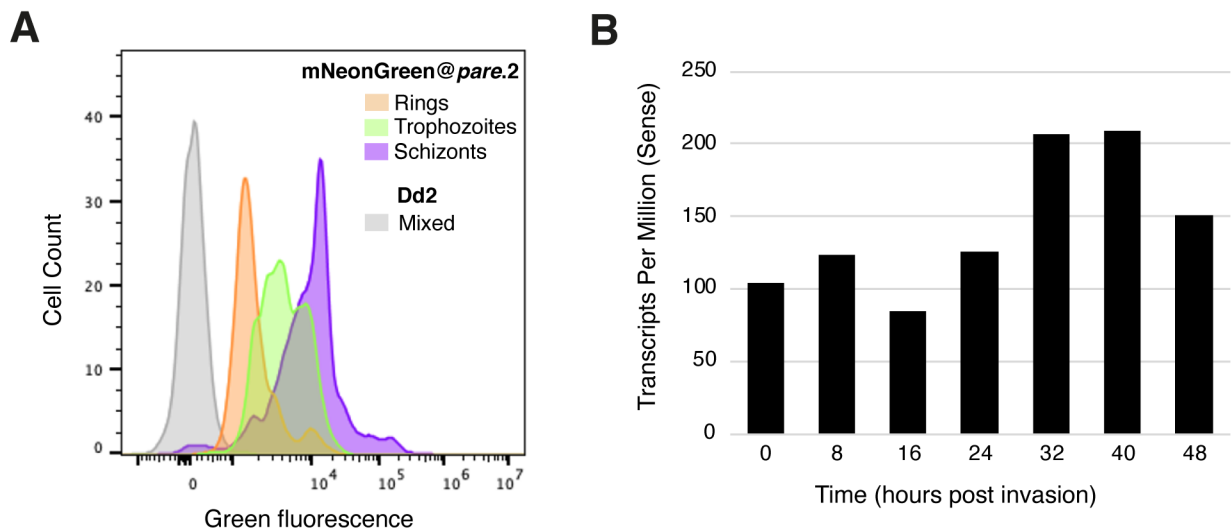


Figure 4

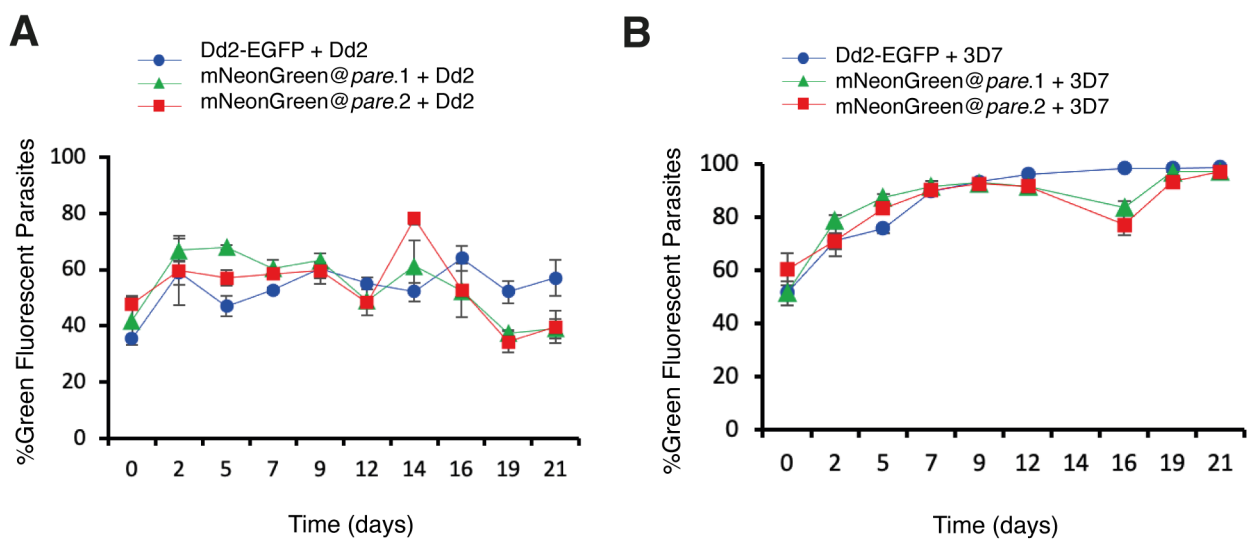


Figure S1

A

3D7	ATGAAGAGCCAGGGTGGAGGAAGATATCGAGGAAGACTCCACAGGTGCGAGCATGCTGAGATGGAAATCCAAATGGATTCT	90
HB3	ATGAAGAGCCAGGGTGGAGGAAGATATCGAGGAAGACTCCACAGGTGCGAGCATGCTGAGATGGAAATCCAAATGGATTCT	90
7G8	ATGAAGAGCCAGGGTGGAGGAAGATATCGAGGAAGACTCCACAGGTGCGAGCATGCTGAGATGGAAATCCAAATGGATTCT	90
GB4	ATGAAGAGCCAGGGTGGAGGAAGATATCGAGGAAGACTCCACAGGTGCGAGCATGCTGAGATGGAAATCCAAATGGATTCT	90
CD01	ATGAAGAGCCAGGGTGGAGGAAGATATCGAGGAAGACTCCACAGGTGCGAGCATGCTGAGATGGAAATCCAAATGGATTCT	90
GA01	ATGAAGAGCCAGGGTGGAGGAAGATATCGAGGAAGACTCCACAGGTGCGAGCATGCTGAGATGGAAATCCAAATGGATTCT	90
IT	ATGAAGAGCCAGGGTGGAGGAAGATATCGAGGAAGACTCCACAGGTGCGAGCATGCTGAGATGGAAATCCAAATGGATTCT	90
Dd2	ATGAAGAGCCAGGGTGGAGGAAGATATCGAGGAAGACTCCACAGGTGCGAGCATGCTGAGATGGAAATCCAAATGGATTCT	90

3D7	TTTCATAATAAGGATGGTTATCTTTAAACCTTATGCATGGACGTTAAAATCCTAGTAGGTGTTATAATAGCATGTCATGGTATGAAT	180
HB3	TTTCATAATAAGGATGGTTATCTTTAAACCTTATGCATGGACGTTAAAATCCTAGTAGGTGTTATAATAGCATGTCATGGTATGAAT	180
7G8	TTTCATAATAAGGATGGTTATCTTTAAACCTTATGCATGGACGTTAAAATCCTAGTAGGTGTTATAATAGCATGTCATGGTATGAAT	180
GB4	TTTCATAATAAGGATGGTTATCTTTAAACCTTATGCATGGACGTTAAAATCCTAGTAGGTGTTATAATAGCATGTCATGGTATGAAT	180
CD01	TTTCATAATAAGGATGGTTATCTTTAAACCTTATGCATGGACGTTAAAATCCTAGTAGGTGTTATAATAGCATGTCATGGTATGAAT	180
GA01	TTTCATAATAAGGATGGTTATCTTTAAACCTTATGCATGGACGTTAAAATCCTAGTAGGTGTTATAATAGCATGTCATGGTATGAAT	180
IT	TTTCATAATAAGGATGGTTATCTTTAAACCTTATGCATGGACGTTAAAATCCTAGTAGGTGTTATAATAGCATGTCATGGTATGAAT	180
Dd2	TTTCATAATAAGGATGGTTATCTTTAAACCTTATGCATGGACGTTAAAATCCTAGTAGGTGTTATAATAGCATGTCATGGTATGAAT	180

3D7	TCTCATGTACGTTAGAATATTAGACATAATGTCGAGGTAGTAAATAATAAGGCATATTAAAAGATGGT	255
HB3	TCTCATGTACGTTAGAATATTAGACATAATGTCGAGGTAGTAAATAATAAGGCATATTAAAAGATGGT	255
7G8	TCTCATGTACGTTAGAATATTAGACATAATGTCGAGGTAGTAAATAATAAGGCATATTAAAAGATGGT	255
GB4	TCTCATGTACGTTAGAATATTAGACATAATGTCGAGGTAGTAAATAATAAGGCATATTAAAAGATGGT	255
CD01	TCTCATGTACGTTAGAATATTAGACATAATGTCGAGGTAGTAAATAATAAGGCATATTAAAAGATGGT	255
GA01	TCTCATGTACGTTAGAATATTAGACATAATGTCGAGGTAGTAAATAATAAGGCATATTAAAAGATGGT	255
IT	TCTCATGTACGTTAGAATATTAGACATAATGTCGAGGTAGTAAATAATAAGGCATATTAAAAGATGGT	255
Dd2	TCTCATGTACGTTAGAATATTAGACATAATGTCGAGGTAGTAAATAATAAGGCATATTAAAAGATGGT	255

B

3D7 TATGATATCTATAGATGAGTTAGCAACGAAACCATCATATAAATTTCTATATCCATTAGCTAATTCTAGGAAGCTTTTTCCAAG 725
 HB3 TATGATATCTATAGATGAGTTAGCAACGAAACCATCATATAAATTTCTATATCCATTAGCTAATTCTAGGA CTTTTTTTCCAAG 725
 7G8 TATGATATCTATAGATGAGTTAGCAACGAAACCATCATATAAATTTCTATATCCATTAGCTAATTCTAGGA CTTTTTTTCCAAG 725
 GB4 TATGATATCTATAGATGAGTTAGCAACGAAACCATCATATAAATTTCTATATCCATTAGCTAATTCTAGGAAGCTTTTTCCAAG 725
 CD01 TATGATATCTATAGATGAGTTAGCAACGAAACCATCATATAAATTTCTATATCCATTAGCTAATTCTAGGAAGCTTTTTCCAAG 725
 GA01 TATGATATCTATAGATGAGTTAGCAACGAAACCATCATATAAATTTCTATATCCATTAGCTAATTCTAGGAAGCTTTTTCCAAG 725
 IT TATGATATCTATAGATGAGTTAGCAACGAAACCATCATATAAATTTCTATATCCATTAGCTAATTCTAGGAAGCTTTTTCCAAG 725
 Dd2 TATGATATCTATAGATGAGTTAGCAACGAAACCATCATATAAATTTCTATATCCATTAGCTAATTCTAGGAAGCTTTTTCCAAG 725

 3D7 TTTACGCTTACTCTGGTTACGTTAATATGTTCCACATATGAATGATTATAGGAATTGATAATTCAATTAAAAACATGT 815
 HB3 TTTACGCTTACTCTGGTTACGTTAATATGTTCCACATATGAATGATTATGAATTGATAATTCAATTAAAAACATGT 815
 7G8 TTTACGCTTACTCTGGTTACGTTAATATGTTCCACATATGAATGATTATGAATTGATAATTCAATTAAAAACATGT 815
 GB4 TTTACGCTTACTCTGGTTACGTTAATATGTTCCACATATGAATGATTATGAATTGATAATTCAATTAAAAACATGT 815
 CD01 TTTACGCTTACTCTGGTTACGTTAATATGTTCCACATATGAATGATTATGAATTGATAATTCAATTAAAAACATGT 815
 GA01 TTTACGCTTACTCTGGTTACGTTAATATGTTCCACATATGAATGATTATGAATTGATAATTCAATTAAAAACATGT 815
 IT TTTACGCTTACTCTGGTTACGTTAATATGTTCCACATATGAATGATTATGAATTGATAATTCAATTAAAAACATGT 815
 Dd2 TTTACGCTTACTCTGGTTACGTTAATATGTTCCACATATGAATGATTATGAATTGATAATTCAATTAAAAACATGT 815

 3D7 AACATGTAGATTAGGTATTAGGTATTAAATGCTATAAAACCTAAATAATGATATGGATTACATTCTGAAAATACACCTATACTTT 905
 HB3 AACATGTAGATTAGGTATTAGGTATTAAATGCTATAAAACCTAAATAATGATATGGATTACATTCTGAAAATACACCTATACTTT 905
 7G8 AACATGTAGATTAGGTATTAGGTATTAAATGCTATAAAACCTAAATAATGATATGGATTACATTCTGAAAATACACCTATACTTT 905
 GB4 AACATGTAGATTAGGTATTAGGTATTAAATGCTATAAAACCTAAATAATGATATGGATTACATTCTGAAAATACACCTATACTTT 905
 CD01 AACATGTAGATTAGGTATTAGGTATTAAATGCTATAAAACCTAAATAATGATATGGATTACATTCTGAAAATACACCTATACTTT 905
 GA01 AACATGTAGATTAGGTATTAGGTATTAAATGCTATAAAACCTAAATAATGATATGGATTACATTCTGAAAATACACCTATACTTT 905
 IT AACATGTAGATTGGTTAGGTATTAGGTATTAAATGCTATAAAACCTAAATAATGATATGGATTACATTCTGAAAATACACCTATACTTT 905
 Dd2 AACATGTAGATTGGTTAGGTATTAAATGCTATAAAACCTAAATAATGATATGGATTACATTCTGAAAATACACCTATACTTT 905

 3D7 TGCTCACTAAAAAAAGATAGTGTATGCTTTTATGGGGTACATTAATTTACACAACTTAAGTGTCTAAAAGAATTATATAC 995
 HB3 TGCTCACTAAAAAAAGATAGTGTATGCTTTTATGGGGTACATTAATTTACACAACTTAAGTGTCTAAAAGAATTATATAC 995
 7G8 TGCTCACTAAAAAAAGATAGTGTATGCTTTTATGGGGTACATTAATTTACACAACTTAAGTGTCTAAAAGAATTATATAC 995
 GB4 TGCTCACTAAAAAAAGATAGTGTATGCTTTTATGGGGTACATTAATTTACACAACTTAAGTGTCTAAAAGAATTATATAC 995
 CD01 TGCTCACTAAAAAAAGATAGTGTATGCTTTTATGGGGTACATTAATTTACACAACTTAAGTGTCTAAAAGAATTATATAC 995
 GA01 TGCTCACTAAAAAAAGATAGTGTATGCTTTTATGGGGTACATTAATTTACACAACTTAAGTGTCTAAAAGAATTATATAC 995
 IT TGCTCACTAAAAAAAGATAGTGTATGCTTTTATGGGGTACATTAATTTACACAACTTAAGTGTCTAAAAGAATTATATAC 995
 Dd2 TGCTCACTAAAAAAAGATAGTGTATGCTTTTATGGGGTACATTAATTTACACAACTTAAGTGTCTAAAAGAATTATATAC 995

 3D7 CTTAGATGACATGGGACACCTTCTACCTATGGAACCTGGAAATGAAAGAGTTCTAAAAAAATTATCACATGGTAGCTGCCATACCCC 1085
 HB3 CTTAGATGACATGGGACACCTTCTACCTATGGAACCTGGAAATGAAAGAGTTCTAAAAAAATTATCACATGGTAGCTGCCATACCCC 1085
 7G8 CTTAGATGACATGGGACACCTTCTACCTATGGAACCTGGAAATGAAAGAGTTCTAAAAAAATTATCACATGGTAGCTGCCATACCCC 1085
 GB4 CTTAGATGACATGGGACACCTTCTACCTATGGAACCTGGAAATGAAAGA TTCTAAAAAAATTATCACATGGTAGCTGCCATACCCC 1085
 CD01 CTTAGATGACATGGGACACCTTCTACCTATGGAACCTGGAAATGAAAGA TTCTAAAAAAATTATCACATGGTAGCTGCCATACCCC 1085
 GA01 CTTAGATGACATGGGACACCTTCTACCTATGGAACCTGGAAATGAAAGA TTCTAAAAAAATTATCACATGGTAGCTGCCATACCCC 1085
 IT CTTAGATGACATGGGACACCTTCTACCTATGGAACCTGGAAATGAAAGAGTTCTAAAAAAATTATCACATGGTAGCTGCCATACCCC 1085
 Dd2 CTTAGATGACATGGGACACCTTCTACCTATGGAACCTGGAAATGAAAGAGTTCTAAAAAAATTATCACATGGTAGCTGCCATACCCC 1085

 3D7 CAAACAAAGAAGAACAA 1101
 HB3 CAAACAAAGAAGAACAA 1101
 7G8 CAAACAAAGAAGAACAA 1101
 GB4 CAAACAAAGAAGAACAA 1101
 CD01 CAAACAAAGAAGAACAA 1101
 GA01 CAAACAAAGAAGAACAA 1101
 IT CAAACAAAGAAGAACAA 1101
 Dd2 CAAACAAAGAAGAACAA 1101
